Modeling of Industrial Nylon-6,6 Polycondensation Process in a Twin-Screw Extruder Reactor. I. Phenomenological Model and Parameter Adjusting

REINALDO GIUDICI,[1] CLÁUDIO AUGUSTO OLLER DO NASCIMENTO,[1] ISABEL CAPOCCHI BEILER,[1] NATÁLIA SCHERBAKOFF[2]

[1] Department of Chemical Engineering, Polytechnic School, University of São Paulo, P.O. Box 61548, 05424-970, São Paulo, SP, Brazil

[2] Rhodia S.A. (Rhône-Poulenc Group), Av. dos Estados, 6144, 09210-900, Santo André, SP, Brazil

Received 9 December 1996; accepted 4 September 1997

ABSTRACT: This article describes a mathematical model for the finishing stage of nylon-6,6 polycondensation in a twin-screw extruder reactor. In the model, the extruder is conceptually divided into two regions. The first one is the partially filled degassing zone, which is operated under low pressure and where the evaporation of water from the polymer takes place. The rate of evaporation is considered to depend on an overall mass transfer coefficient and is limited by the water–polymer physical equilibrium. In the second region, which is fully filled, the polymer flow is assumed to be plug-flow and, in this region, the reversible polycondensation reaction occurs, as well as degradation reactions. A comparison with experimental data obtained in an industrial plant shows fairly good agreement with model predictions after optimal fitting of the rate coefficients. © 1998 John Wiley & Sons, Inc. J Appl Polym Sci **67:** 1573–1587, 1998

Key words: mathematical model; nylon-6,6 polymerization; twin-screw extruder; reactive extrusion

INTRODUCTION

Nylon-6,6 polymer is produced from hexamethylene diamine and adipic acid monomers. Like many other step-growth polymerization processes, nylon-6,6 polycondensation is carried out typically in three stages due to different conditions of kinetic, mass and heat transfer, condensate removal, and viscosity in each process stage.

The design of the finishing stage reactors requires special features since they usually operate with high viscosity polymers, thus under difficult conditions of condensate removal and heat transfer. Extruder reactors can be effective in handling these conditions, as described in reviews on reactive extrusion.[1–3]

The kinetics and equilibrium of nylon-6,6 polymerization were studied by Ogata.[4,5] Other researchers, such as Kumar et al.[6,7] and Steppan et al.,[8] have proposed different kinetic expressions, but all of them have strongly based their equations on Ogata's data. Steppan et al.[9] also presented a kinetic model for degradation reactions in this system. It should be emphasized that all the aforementioned works refer to the noncatalyzed nylon-6,6 polymerization. The effect of catalyst on the kinetics of this process under typical industrial conditions has not been reported yet.

Most works on modeling of nylon-6,6 finishing reactors have focused primary on thin or wiped

Correspondence to: R. Giudici (rgiudici@usp.br).

Journal of Applied Polymer Science, Vol. 67, 1573–1587 (1998)
 CCC 0021-8995/98/091573-15

film reactors (Steppan et al.[10]; Choi and Lee[11]). Jacobsen and Ray[12,13] presented a unified general framework for the kinetic modeling of polycondensation reactions. Later, Hipp and Ray[14] applied this general framework in a dispersion model for tubular reactors, which is able to represent a number of different reactor types, including rotating disk reactors and twin-screw extruder reactors.

Comprehensive models for conventional plasticating extruders have been developed, for example, by Tadmor and Gogos,[15] Meijer and Elemans,[16] Vincelette et al.[17] More recently, there has been a growing interest in the use of extruders as continuous flow reactors for both synthesizing and modifying polymers.[1,3] As a consequence, a number of works have described the modeling of screw reactors with different levels of complexity. Siadat et al.[18] discussed the basic features of a simple model for a polycondensation reaction in an extruder reactor. They concluded that the extruder behaves nearly like a plug-flow reactor. For the modeling of the reactive extrusion process, Michaeli et al.[19] suggested a combination of the residence time, obtained by calculation or measurement, with the reaction kinetics and an approximation for the flow pattern in the reactor, such as a cascade of CSTRs or pipe reactors. Michaeli et al.[19] claim that "it is absolutely possible to use the simpler pipe reactor as a basis for the preliminary design of polymerization zone of screw reactor." Several authors have accounted for deviations from plug-flow behavior using a combination of the kinetics and the residence time distribution (Michaeli et al.,[19] Maier and Lambla,[20] Tzoganakis et al.[21]).

Several different applications have been reported in the scientific and patent literature on reactive extrusion.[1,3] To mention only a few examples, one can point out applications to peroxide degradation of polypropylene in single screw extruder[21]; bulk polymerization of *n*-butylmethacrylate and copolymerization with 2-hydroxypropylmethacrylate[22,23]; anionic polymerization of nylon-6, of nylon-6 block copolymers, and of polystyrene[19]; and esterification grafting of nonylphenyl-ethoxylate onto a premaleated ethylene–propylene rubber[20] in twin-screw extruders. To the authors' best knowledge, no application regarding the modeling of the twin-screw extruder reactor for nylon-6,6 polycondensation has been reported previously.

The main aim of this article is to describe the modeling of the finishing stage of an industrial process of nylon-6,6 polycondensation in a twin-screw extruder reactor. The model is validated by comparison with industrial data under catalyzed conditions.

MATHEMATICAL MODEL

In mathematical modeling, a concern always present is the adequate balance between sophistication and simplification. Rigorous modeling of the fluid mechanics and its interactions with other phenomena in the extruder can be extremely complex.[1] The guideline followed in the present work was to propose a model whose complexity could be checked against plant data. Therefore, it is useful to consider several aspects of the idealization of the flow in the extruder.

The process under study, the post-condensation of nylon-6,6, is carried out in a self-wiping, co-rotating, twin-screw extruder. The extruder is fed with polymer melt. Two zones can be distinguished in the extruder as follows: a partially filled zone, in which the channels are not completely filled with polymer, and a fully filled zone. In the first section of the extruder, there is a vacuum vent port that promotes degassing conditions for water evaporation. It is followed by a second section in which the main phenomenon is the polycondensation reaction, during which much less or no evaporation takes place.

The above considerations prompted us to adopt a two-region model for the extruder. Thus, in the model, water evaporation is considered to take place only in the first region (Region I), with no reaction in this section. A kinetic approach is used to model the mass transfer so that the water content in the polymer that leaves this section is a function of the pressure imposed by the vacuum system, the temperature, and the residence time in this region. On the other hand, in the second section (Region II), it is assumed that only chemical reactions occur, with no further evaporation taking place. Plug-flow is assumed in Region II. In the literature on reactive extrusion, the plug-flow hypothesis has been used as a reasonable approximation for a co-rotating, twin-screw extruder,[2] as well as for a single-screw extruder.[18] As pointed out by Biesenberger,[24] ". . . the extruder tends to be more plug-like than the tube in laminar flow, owing to the presence of transverse convection in the channels . . . self-wiping flights

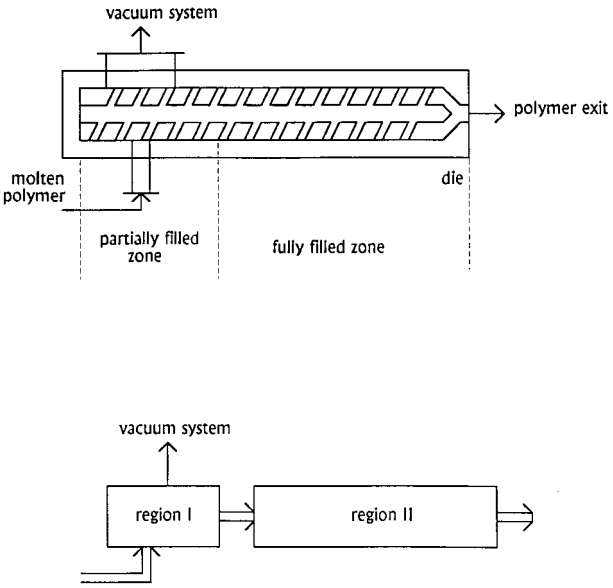

Figure 1 Scheme of the two-region model for the extruder–reactor.

are believed to impart even more plug-like behavior to co-rotating twin screw extruders with tightly intermeshing screws." In addition, the extruder is considered to operate isothermally.

Figure 1 illustrates the two-region model for the extruder.

Model Equations for Region I

Water evaporation is the only phenomenon considered in Region I. The mass transfer rate of water evaporation at the vacuum vent port was expressed as a function of an overall mass transfer coefficient and a driving force based on the extent of departure from water–polymer equilibrium. The balance equation for water in polymer (considering plug-flow in Region I) is given by

$$Q\frac{dC_w}{dV} = -ka(C_w - C_{w,eq}) \quad (1)$$

where Q is the volumetric flow rate of polymer, k is an effective mass transfer coefficient, and a is the mass transfer area per unit volume of polymer. Assuming constant conditions, eq. (1) can be integrated over the volume of polymer in Region I to give

$$C_w = C_{w,eq} + (C_{w,o} - C_{w,eq})\exp\left[-ka\frac{V_I}{Q}\right] \quad (2)$$

where $C_{w,o}$ is the water concentration in the feed polymer (assumed to be in chemical equilibrium with the polymer), and V_I is the volume of polymer in Region I. Note that if the value of the mass transfer coefficient becomes high enough, the water content approaches the equilibrium concentration. Therefore, this kinetic approach for water evaporation accounts for an equilibrium situation as an asymptotic case.

The solubility of water in molten nylon-6,6 was calculated as a function of temperature and pressure from the correlation given by Ogata[4] as follows:

$$C_{w,eq} = 2C_tP10^{(3050/T-10{,}09)} \quad (3)$$

where P is the pressure in mmHg and T is the temperature in degrees Kelvin.

Model Equations for Region II

The mass balances for the various species are given by

$$Q\frac{dC_i}{dV} = \sum_{j=1}^{m}\alpha_{i,j}R_j \qquad i = A, C, L, W, SE, SB, X \quad (4)$$

where $\alpha_{i,j}$ is the stoichiometric coefficient of species i in reaction j, and R_j is the rate of reaction j. The species considered are amine end-group (A), carboxyl end-group (C), amide linkage (L), water (W), stabilized end-group (SE), Schiff base (SB), and crosslink (X). The reaction considered are polycondensation and four degradation reactions. The reaction scheme and the corresponding kinetics were taken from the work of Steppan et al.[8,9] and are presented in the Appendix.

The number-average molecular weight can be obtained from

$$M_n = 2\rho/(C_A + C_C + C_M + C_{SE} + C_{SB} - C_X) \quad (5)$$

where C_M is the concentration of monofunctional monomer added to the formulation and ρ is the polymer density.

As initial conditions for eq. (4), the concentrations of the species at the inlet of the region II are

the concentrations at the exit of Region I [the water concentration is calculated by eq. (2), and the concentration of the other species are the same as those at the inlet of the extruder]. Equation (4) is numerically solved for the region II using an adequate marching technique (standard variable-step Runge–Kutta–Gill method) to obtain the concentration of the species along the extruder.

Empirical Correlation for the Relative Viscosity

In industrial practice, the relative viscosity (RV) is probably the most important variable since this property is used to characterize the quality of the polymer produced in the post-condensation process. However, the balance equations predict only the concentration of end groups. Therefore, it was necessary to include an equation for RV as a function of the concentrations included in the model balance equations. As a first attempt, this was done through an empirical equation between the relative viscosity and the number-average molecular weight M_n (in part II of this series,[25] an improved relation based on neural networks it is presented).

A set of 522 experimental data of relative viscosity along with the corresponding experimental values of amine and carboxyl end-group concentrations was used to develop this empirical relation. Note that the amine and carboxyl end groups were the only concentrations measured to evaluate M_n so that it was not possible to consider, at this point, the other end groups shown in eq. (5). This simplified analysis lead to an empirical relation of the following form:

$$RV = \beta M_n \tag{6}$$

Figure 2 shows the comparison between eq. (6) and the data. Most of data are within ±5% of the prediction. This spread may be due to process variations, polymer degradation, and, as already pointed out, the noninclusion of other end groups.

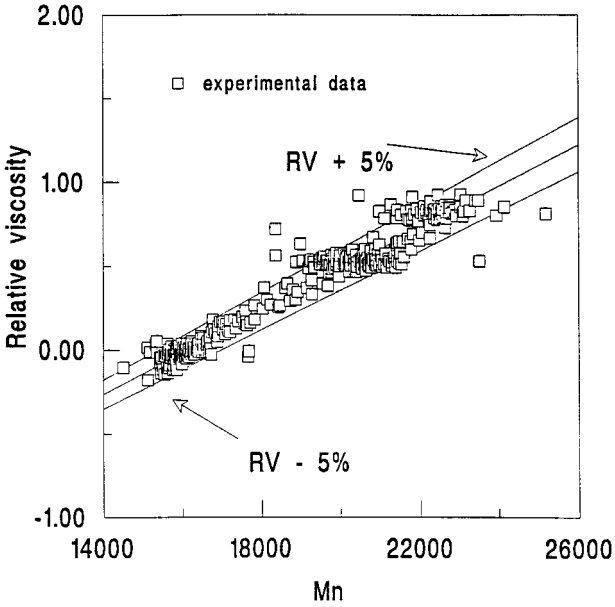

Figure 2 Parity plot for the empirical correlation for the relative viscosity.

EXPERIMENTAL PLANT DESIGN

Preliminary analysis of industrial operation data showed that the following operation variables are important: the extruder temperature, the pressure of the vacuum system, the flow rate, the pressure at the extruder head, and the screw rotation speed. Other variables were the relative viscosity and the amine and carboxyl end-group concentrations at the entrance of the extruder and at the spirenette after the extruder.

Application of experimental design to acquire data in an industrial plant is more complex than in laboratory experiments. A change of process variables can lead to product outside of specifications, resulting in losses of thousands of dollars. It is also not possible to open all the control loops and operate the system by hand. These two points should be taken in account very carefully. In general, historical plant data do not give enough information far from the normal operating conditions because the operation range is usually very narrow. Sometimes historical disaster operations give us good information about the process and about which variables we should search.

In order to get data for model validation, a planned set of 23 experiments was performed in the industrial plant. The experimental plan consisted, at first, of an incomplete factorial design, complemented with some additional experiments and triplicate runs at the central point. In the industrial practice, however, some combinations of variables were not possible due to operational constraints,[26] so the final experimental runs were not exactly as shown in Table I.

Table I Coded Experimental Plan

Run	T	Pv	Ph	Q	RPM
2	−1	−1	−1	−1	+1
3	+1	−1	−1	−1	+1
4	−1	+1	−1	−1	−1
5	+1	+1	−1	−1	−1
6	−1	−1	+1	−1	−1
7	+1	−1	+1	−1	−1
8	−1	+1	+1	−1	+1
9	+1	+1	+1	−1	+1
10	−1	−1	−1	+1	−1
11	+1	−1	−1	+1	−1
12	−1	+1	−1	+1	+1
13	+1	+1	−1	+1	+1
14	−1	−1	+1	+1	+1
15	+1	−1	+1	+1	+1
16	−1	+1	+1	+1	−1
17	+1	+1	+1	+1	−1
1	0	0	0	0	0
18	0	0	0	0	0
23	0	0	0	0	0
19	0	−1	0	0	0
20	0	+1	0	0	0
21	0	0	0	0	+1
22	0	0	0	0	−1

Residence Time Measurements

One critical point for the model application is the knowledge of the residence time of the polymer in the extruder. The extruder normally does not operate fully filled, allowing the presence of a partially filled zone where evaporation of water takes place. The evaporation of water produces the driving force for the polycondensation in the subsequent fully filled zone. The extent of the partially filled zone may vary with the operating conditions. Because of the partial filling, the residence time is not precisely known. The knowledge of the degree of filling is very important because the extent of the partially filled zone affects the space time of the polymer, with implications for the degree of polymerization. Moreover, if the conditions are such that the extruder becomes completely filled, there will be no place for evaporation, dramatically changing the process response. Therefore, it is extremely important to predict the residence time or, alternatively, the degree of filling.

Although no direct measurement of the residence time was possible in the extruder, an estimate was obtained from a specially planned procedure. Table I presents the coded experimental plan of the industrial runs.

In each run of Table I, the following procedure was carried out. After setting the independent variables shown in Table I and waiting for the process to reach the steady state, the vacuum system was suddenly turned off. Thereafter, degassing no longer occurs, so that no driving force for polycondensation is generated. After the vacuum shutdown, the polymer that enters the extruder will not increase its degree of polymerization. When this lower viscosity polymer reaches the spinnerets at the end of the extruder, the pressure drop in the spinneret pack will decrease. The time elapsed to change the pressure drop in the spinnery pack gives an estimate of the polymer residence time in the system.

A typical pressure drop response at the spinnery pack is showed schematically in Figure 3. The figure also illustrates the procedure used to estimate the average residence time.

Of all the 23 runs in Table I, only runs 16 and 17 presented an abnormal operation. In these runs, change in the pressure drop at the spinneret pack was observed, an indication of flooding of the extruder, that is, of a fully filled extruder with no room for water evaporation. More details of these transient experiments in the extruder are discussed elsewhere by Giudici et al.[26]

MODEL VALIDATION

To check the model predictions, a set of 21 experiments (all except runs 16 and 17) performed in an industrial plant was used. The runs cover a wide range of process variables, such as barrel temperature, vacuum applied to the degassing zone, flow rate, pressure at the extruder head, and screw rotation speed.

In order to validate the model and make its predictions quantitatively reliable, it was found to be necessary to fit the model to industrial data by adjusting three model parameters, namely, the effective mass transfer coefficient (and area) of water evaporation (ka), a correction factor for the polycondensation reaction (f_c), and a correction factor for the degradation reactions (f_d). The first parameter defines the effective kinetics of water evaporation in the extruder. The correction factors account for the presence of catalyst in the industrial process

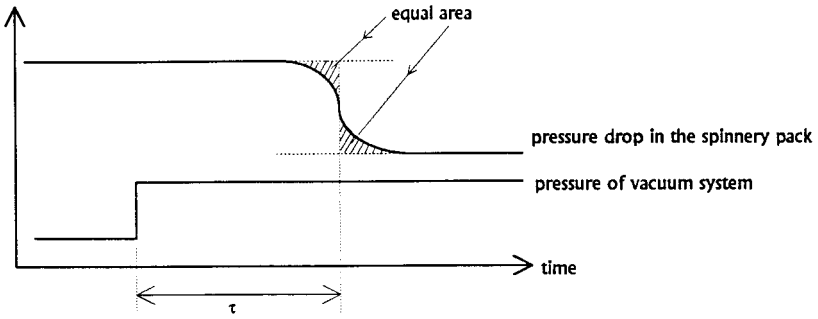

Figure 3 Typical response of pressure drop in the extruder.

that is not considered in the kinetic models taken from the open literature.

The parameters were estimated by minimizing the following nonlinear least-squares criterion involving the differences between model predictions and experimental values of the concentrations of amine (C_A) and concentration of carboxyl (C_C) end groups, as follows:

$$\min[S] = W_A \sum_{i=1}^{n} \left(\frac{C_{Ai} - \hat{C}_{Ai}}{C_{Ai}} \right) + W_C \sum_{i=1}^{n} \left(\frac{C_{Ci} - \hat{C}_{Ci}}{C_{Ci}} \right)^2 \quad (7)$$

where the caret symbol (ˆ) stands for the calculated values.

The weighting factors were chosen as $W_A = W_C = 1$. For the minimization of the criterion given by eq. (7), the routine UNCMND from the book of Kahaner et al.[27] was used.

Relative viscosity is not included in the objective function [eq. (7)] due to the uncertainty in the empirical correlation used to predict it (relative viscosity is not a primary prediction of the model).

Model Adjusting without Degradation Reactions

The first attempt was to fit the model without considering the degradation reactions. In this case, the model has only two adjustable parameters (ka and f_c) to be adjusted. A systematic deviation in the predictions showed that the model was not satisfactory. This conclusion was also confirmed by a statistically based F-test of adequacy,[28] in which the model was rejected at 95% confidence level.

Model Adjusting Considering the Degradation Reactions

The analysis of the experimental data shows that the consumption of amine and carboxyl end groups in the industrial post-condensation process is different, as shown in Figure 4. This is an indication of the presence of degradation reactions in the process since the stoichiometry of the amidation reaction implies that the consumptions should be equal. Since degradation

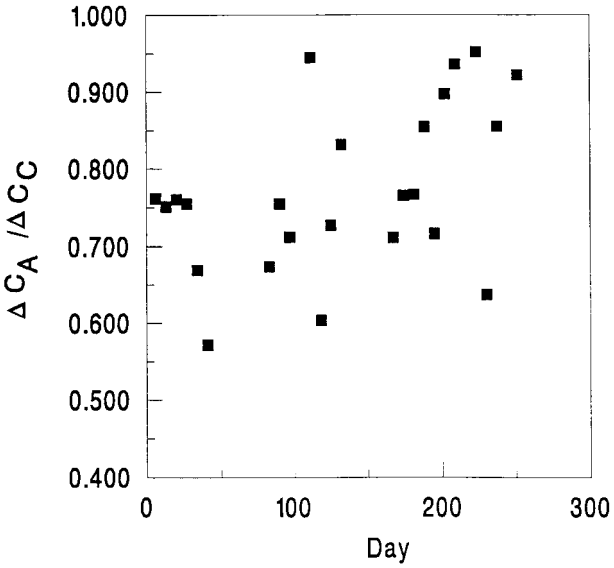

Figure 4 Ratio of consumption of amine and carboxyl end groups as a function of operation days.

Table II Parameter Summary

	Estimated Parameter	Standard Deviation	t-Value
$ka(s^{-1})$	0.09	0.04	2.2
f_c	15.44	2.42	6.4
f_d	3.67	0.24	15.4

Elements of the Correlation Matrix of the Parameters

	ka	f_c	f_d
ka	1	−0.521	+0.021
f_c	−0.521	1	+0.044
f_d	+0.021	+0.044	1

Residue, $S = 79.65$; number of points, N = 21 × (2 variables) = 42; number of parameters, $p = 3$; degrees of freedom, $N - p = 39$; variance, $s^2 = S/(N - p) = 2.04$; standard deviation, $s = 1.43$.

may change the concentration of amine and carboxyl end groups by different amounts, the inclusion of degradation reactions allows for taking these experimental observations into account in the model. Indeed, inclusion of degradation reactions resulted in a much better fit than in the previous case, with equally distribution in both positive and negative deviations between model predictions and experimental measurements. Table II summarizes the estimated parameters and standard deviations.

The model was able to represent adequately the industrial extruder data. Figure 5 presents the comparison between predictions and experimental plant data. The adequacy of the model for the prediction of amine and carboxyl end-group concentrations was also confirmed by a statistically based F-test of adequacy.[28]

It is noteworthy that the behaviour observed in runs 16 and 17 is correctly predicted, even though these runs were not used in the fitting. They correspond to the points of highest end-group contents in Figure 5. For these runs, it was supposed that the extruder was flooded, so that no water evaporation could take place. This result is an additional validation for the main hypothesis of the model, namely, the separation into two zones.

The observed deviations in relative viscosity may be ascribed to the empirical correlation used to evaluate RV from the average molecular weight calculated from the model. The main problem in the empirical correlation used to predict the RV values is that the polymer is assumed to be linear, which might not necessary be true if degradation occurs. Note that although RV is not a primary prediction of the model, it is an important industrial variable since it is used for quality control of the polymer. Therefore, further efforts should be directed toward improving the prediction of this variable.

AVERAGE RESIDENCE TIME PREDICTION

In order to make the model useful for optimization studies, it is necessary to obtain acceptable predictions for the length of the fully filled reaction zone or, equivalently, the average residence time in the reaction zone.

For this prediction, we made use of a simple model for the flow in an extruder. This flow model is the so-called screw pump model or continuous drag flow model.[24,15,16,22] For the fully filled zone, the flow is given by the sum of the effects of the drag flow and the pressure flow in the form as follows:

$$Q = (2m - 1)\frac{\pi DWH}{2} F_d N_r \cos\phi + (2m - 1)\frac{WH^3}{12\eta}\left(-\frac{dP}{dz}\right)F_p \quad (8)$$

where m is the number of thread starts, H is the channel depth, W is the channel width, D is the barrel diameter, ϕ is the pitch angle, N_r is the screw rotation rate, η is the melt viscosity, dp/dz is the pressure gradient in channel direction, and F_d and F_p are shape factors for the drag and pressure flow, respectively. Since there is no axial pressure gradient in the partially filled zone, the appropriate boundary conditions for eq. (8) are

$$P = P_v \quad \text{at } z = z_1 \quad (9)$$

$$P = P_h \quad \text{at } z = L \quad (10)$$

where z_1 is the length of the partially filled zone and L is the total length of the extruder.

Applying eq. (8) for the whole fully filled zone leads to

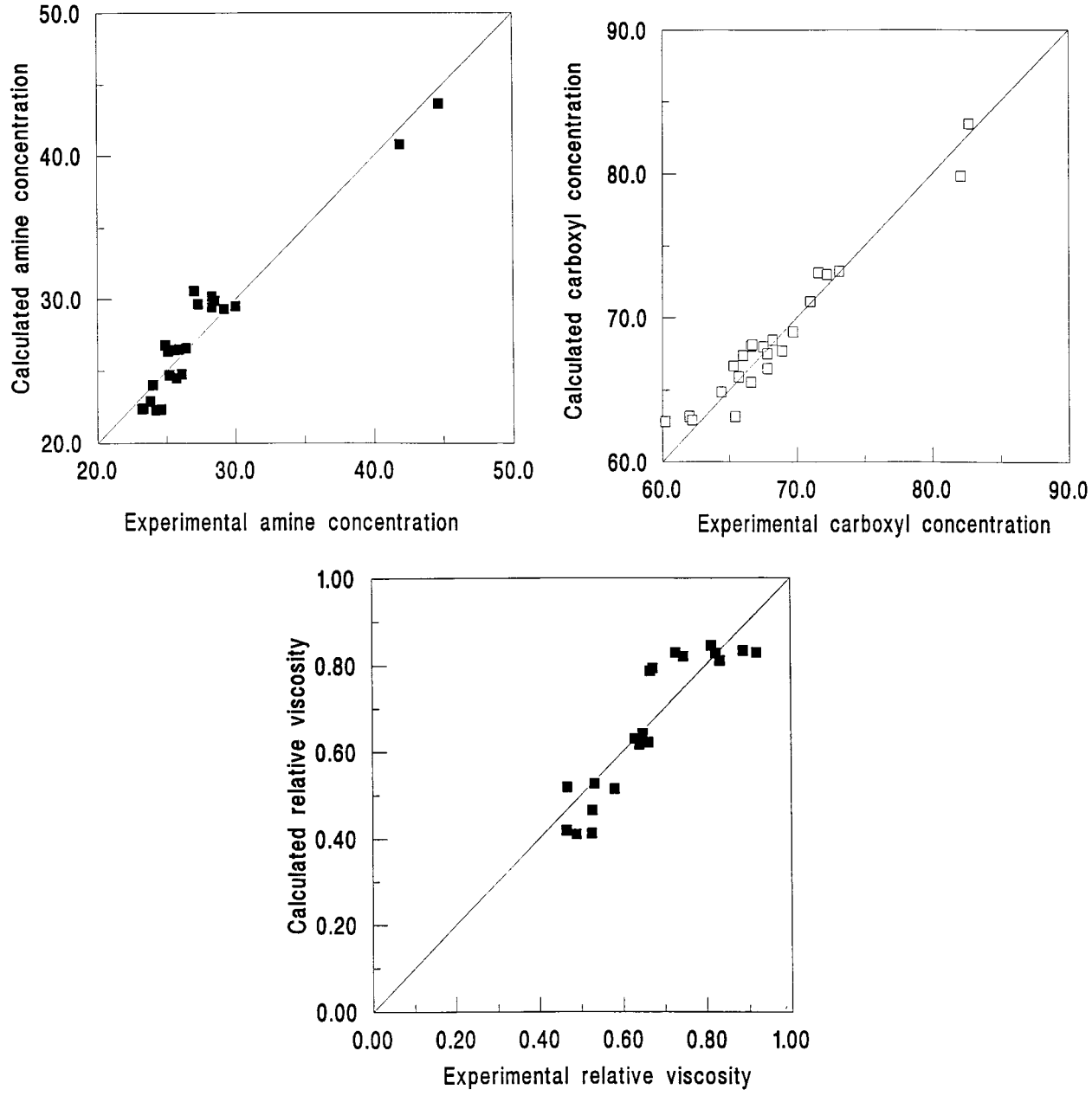

Figure 5 Comparison between predictions and experimental plant data.

$$Q = K_1 N_r - K_2 \frac{(P_h - P_v)}{\langle \eta \rangle (L - z_1)} \tag{11}$$

where K_1 and K_2 are adjustable parameters (including geometric parameters), and $\langle \eta \rangle$ is an average melt viscosity of the polymer along the extruder. Equation (11) was then used as the basis of a semitheoretical relation in which K_1 and K_2 are treated as fitting parameters, and $\langle \eta \rangle$ is an empirical function of the operation conditions.[26] The average residence time (in region II) can be evaluated by

$$\tau = \frac{V_{II}}{Q} = \frac{(L - z_1)A}{Q} \tag{12}$$

where A is the cross-section area for flow in the extruder. The predictions of eqs. (11) and (12) are

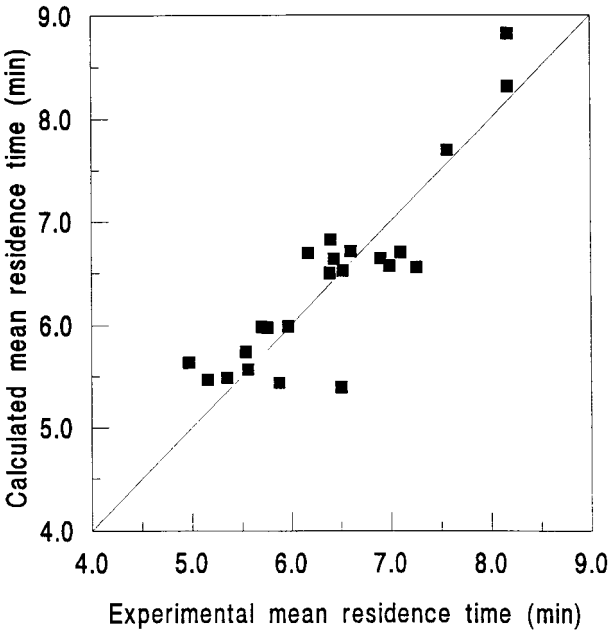

Figure 6 Parity plot for the average residence time.

compared with the experimental data in Figure 6. This practical approach allows one to calculate the length of the fully filled zone and then the average residence time of polymer in the reaction zone.

SIMULATION RESULTS

The overall structure of the model is presented schematically in Figure 7. It consists of the following four main steps.

1. The calculation starts with the evaluation of the lengths of region I (z_1) and of region II ($L - z_1$), using eq. (11).
2. Equation (2) is then used to simulate the water evaporation in region I.
3. The water concentration at the end of region I and the concentrations of the other components in the feed are employed as initial conditions for the ordinary differential equations [eq. (4)] that represent the model for region II. These equations are numerically solved by a standard variable-step Runge–Kutta–Gill subroutine.
4. The concentrations of all components at the extruder exit are then used for the evaluation of relative viscosity, using eqs. (5) and (6).

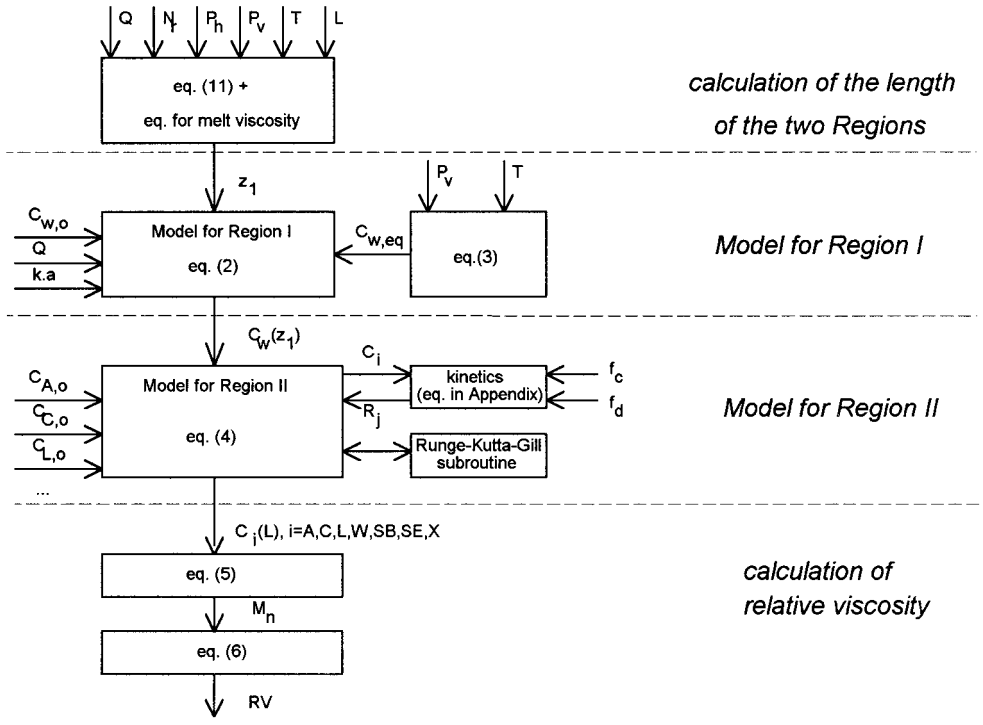

Figure 7 Schematic representation of the mathematical model.

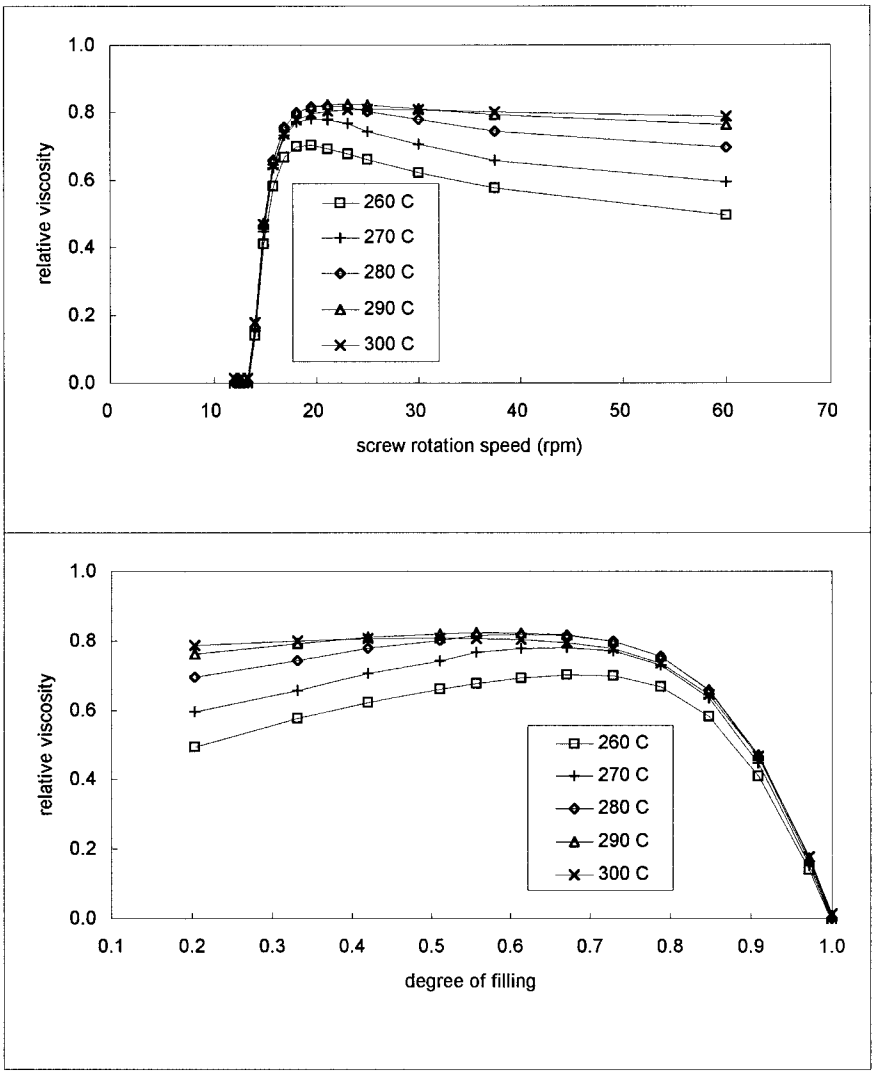

Figure 8 Effect of temperature and screw rotation speed on the relative viscosity as predicted by the model.

Figure 8 shows the effect of temperature and screw rotation on the relative viscosity. When the other variables are kept constant, the screw rotation defines the degree of filling (also shown in Fig. 8), defined here as the ratio of the filled length to the total length. For a given temperature, relative viscosity passes through a maximum with respect to the degree of filling. This maximum is a consequence of two opposing effects: increasing the degree of filling increases the residence time in region II, while the volume of region I decreases. For degree of filling lower than about 0.7, the evaporation of water almost reaches equilibrium at the end of region I so that an increase in the degree of filling improves the polymerization by increasing the residence time in region II. However, excessively high values of the degree of filling can cause an opposite effect by decreasing the volume of region I (where the water is removed). In the limit of a flooded extruder (degree of filling equals 1), no water evaporation occurs; thus, the relative viscosity of the polymer at the extruder exit dramatically decreases, approaching the value of the *RV* of the polymer feed (the values of *RV* were coded with reference to the polymer feed so that the coded *RV* of the polymer feed is zero). Raising the temperature from 260 up to 290°C can increase *RV*, but a further

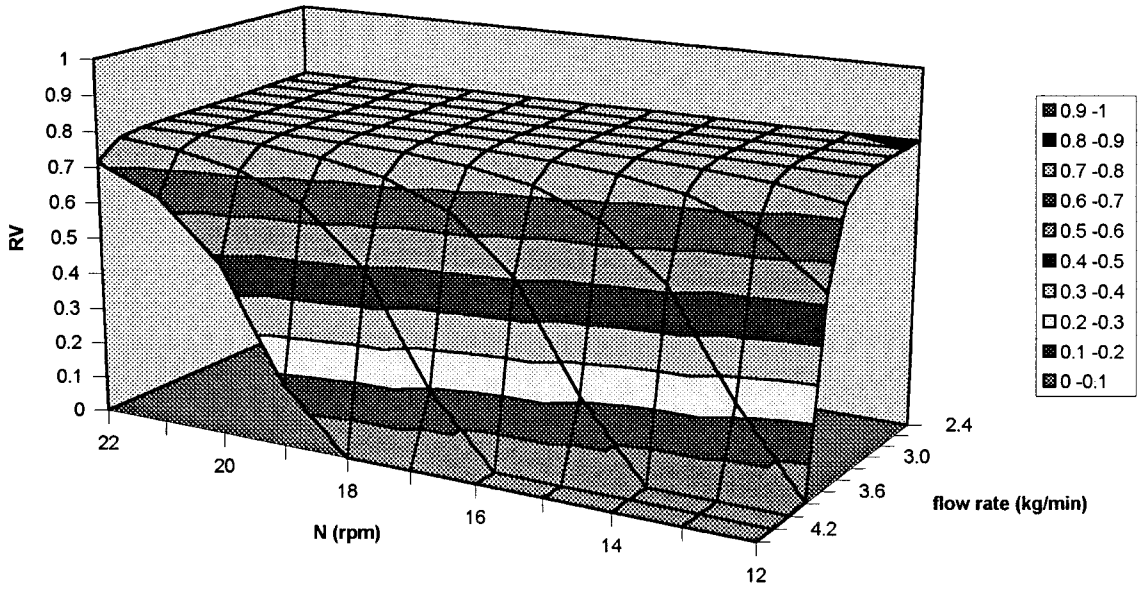

Figure 9 Effect of flow rate and screw rotation speed on the relative viscosity as predicted by the model.

temperature increase is not effective due to the effect of the degradation reactions.

Figure 9 shows the effects of screw rotation speed and flow rate on the relative viscosity of the polymer produced. There is a range of variation of these two variables in which the relative viscosity is high and almost constant. However, the combination of high flow rates and low screw rotation speeds causes a strong decrease in the degree of polymerization, and the relative viscosity approaches the value of RV of the polymer feed. This corresponds to a flooding of the extruder (the degree of filling approaches 1.0). In addition, each horizontal curve in Figure 9 defines the range of flow rate and screw rotation that produces a given RV. The steepness of the surface also indicates the sensitivity of the steady state, information useful for control and stability studies. Note that in the industrial process under consideration, the flow rate is defined by the production and imposed by positive displacement pumps, while the screw rotation speed can be used to control the residence time (and degree of filling) within certain limits. Figure 9 is a good example of how to use the model predictions to determine the feasible range of operation variables. For instance, this figure shows that it is possible to increase the production (flow rate) of polymer and retain almost the same quality (relative viscosity) by operating the extruder at a higher screw rotation speed.

Figure 10 shows the effect of the vacuum pressure. Relative viscosity can be raised significantly by lowering the vacuum pressure. The use of lower vacuum pressure causes an increase in the degree of polymerization since more water is evaporated in region I, enhancing the driving force for polymerization.

The model was used to study the feasibility of increasing the production (that is, flow rate) for a given desired grade (represented by the relative viscosity) by selecting adequate values of the operation variables (temperature, vacuum pressure, screw rotation). No changes in the equipment or in the quality of the feed polymer were considered. Taking into account the constraints of the industrial plant, the simulations indicated the potential of increasing production by about 20 to 25% just by selecting a better operation point. Additional experiments confirmed that these predictions were correct, and the feasible production enhancement was indeed accomplished.

CONCLUSIONS

A model for nylon-6,6 polymerization in an extruder reactor is presented and validated using industrial data. The effect of the catalyst was accounted for by adjusting parameters of the kinetic model taken from the literature. In addition, the

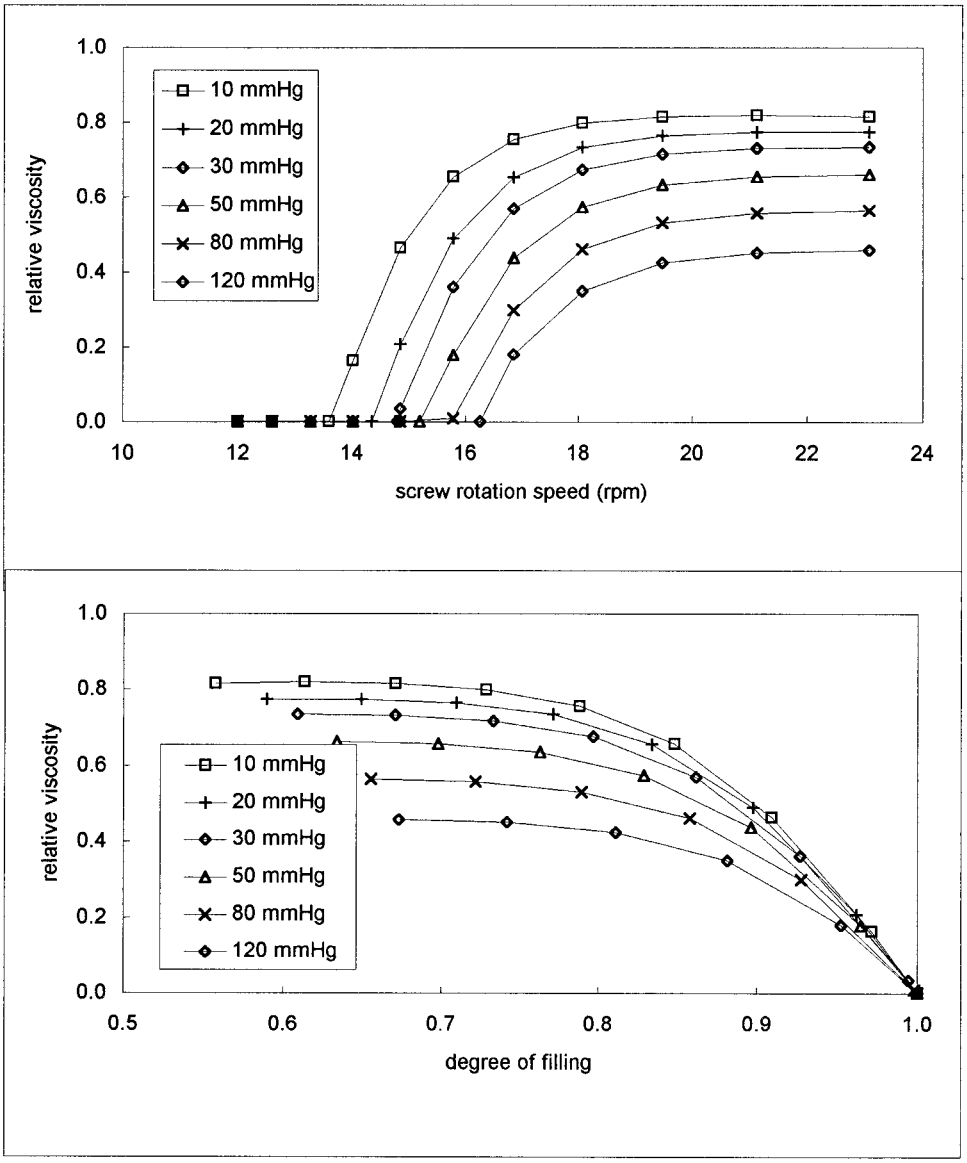

Figure 10 Effect of vacuum pressure and screw rotation speed on the relative viscosity as predicted by the model.

mass transfer coefficient for water evaporation in the region near the vacuum vent port was also estimated by fitting the model.

The model is satisfactory for studying the feasibility of process modifications. The model has proved to be useful for obtaining a 20% increase in the plant production and accurately predicts the amine and carboxyl end-group concentrations over the industrial variable range examined.

The relative viscosity is predicted reasonably well, through an empirical correlation from the amine and carboxyl end-group concentrations calculated by the model. The accuracy of this correlation is within 5% of the experimental values. Further improvements of the *RV* prediction are discussed in the companion article (part II of this sequence).[25]

The authors thank Rhodia S.A. (Rhône Poulenc Group) for supporting this work and Prof. Frank Quina for revising the manuscript. Also partial support from FAPESP, CNPq, and CAPES is gratefully appreciated.

APPENDIX

Kinetics of Polycondensation

The polycondensation of nylon-6,6 in Region II was treated as a reversible reaction between amine (A) and carboxyl (C) end groups to form an amide linkage (L) with the elimination of a water molecule (W):

$$A + C \rightarrow L + W \quad (r1)$$

Experimental data on the kinetics and equilibrium for the nylon-6,6 polycondensation are rare in the open literature. To our knowledge, the only published data on this subject are in the papers by Ogata.[4,5] Other researchers such as Kumar et al.[6,7] and Steppan et al.[8] have also proposed different expressions for the kinetics, but they have based their investigations on Ogata's data. In the present work, the equations presented by Steppan et al.[8] are used along with a correction factor f_c that was fitted to account for the effect of catalyst present in the industrial process. According to those authors,[8] these equations are valid for the water concentration range of 1 to 90% and for temperatures from 200 to 265°C, in the following form:

$$R_1 = C_t k_1 (x_A x_C - x_L x_W / K_{app}) \quad (A.1)$$

where

$$k_1 = k_{1,0} \exp\left[-\frac{E_{ap}}{R}\left(\frac{1}{T} - \frac{1}{T_0}\right)\right] \quad (A.2)$$

$$k_{1,0} = \exp\{2.55 - 0.45 \tanh[25(x_w - 0.55)]\} + 8.58\{\tanh[50(x_w - 0.10)] - 1\} \times 1 - 30.05x_c) \quad (A.3)$$

$$K_{app} = K_0 \exp\left[-\frac{\Delta H_{app}}{R}\left(\frac{1}{T} - \frac{1}{T_0}\right)\right] \quad (A.4)$$

$$K_0 = \exp\{[1 - 0.47 \exp(-x_w^{1/2}/0.2)] \times (8.45 - 4.2x_w)\} \quad (A.5)$$

$$\Delta H_{app}/R = \{7650 \tanh[6.5(x_w - 0.52)] + 6500 \exp(-x_w/0.065) - 800\}/1.987 \quad (A.6)$$

Kinetics of Degradation Reactions

Steppan et al.[9] have also proposed a simplified kinetic scheme that is able to explain the main features observed in a number of previously published data on the degradation of nylon-6,6. In the present model, the degradation reactions were considered through their kinetic scheme,[9] which includes reactions producing volatile species such as ammonia and carbon dioxide, as well as crosslinkages, as follows.

$$C \rightarrow SE + W \quad (rd1)$$

$$L \rightarrow SE + A \quad (rd2)$$

$$SE \rightarrow SB + CO_2 \quad (rd3)$$

$$SB + 2A \rightarrow X + 2NH_3 \quad (rd4)$$

where SE refers to a stabilized (or cyclized) end group, SB to a Schiff base, and X to a crosslink. The kinetics of degradation were calculated by the following equations[9]:

$$R_{d1} = C_t k_{d1} x_C \quad (A.7)$$

$$R_{d2} = C_t x_L (k_{d2} + k_{d2,c} x_A) \quad (A.8)$$

$$R_{d3} = C_t k_{d3} x_A x_{SE}^{0.1} \quad (A.9)$$

$$R_{d4} = C_t k_{d4} x_A x_{SB}^{0.3} \quad (A.10)$$

where

$$x_i = C_i/C_t \quad i = A, C, L, W, SE, SB, X \quad (A.11)$$

$$C_t = C_A + C_C + C_L + C_W + C_{SE} + C_{SB} + C_X \quad (A.12)$$

$$k_j = k_{j0} \exp\left[\frac{-E_j}{R}\left(\frac{1}{T} - \frac{1}{T_0}\right)\right] \quad (A.13)$$

The kinetic parameters for the degradation are presented in Table AI. Steppan et al.[9] have shown that the reaction system of polycondensation and degradation is valid for temperatures up to 305°C.

Table A.I Kinetic Parameters for Nylon-6,6 Degradation, after Steppan et al.[9]

Reaction	Rate Constant	k_0 (L/h)	E (cal/mol)	T_0 (K)
R_{d1}	k_{d1}	0.06	30,000	293
R_{d2}	k_{d2}	0.005	30,000	305
R_{d2} (catalyzed)	$k_{d2,c}$	0.32	30,000	305
R_{d3}	k_{d3}	0.35	10,000	305
R_{d4}	k_{d4}	10.0	50,000	305

In the present article, a correction factor f_d was fitted to account for the effect of catalyst on the degradation reactions.

NOMENCLATURE

a	mass transfer area for water evaporation in Region I per unit volume (m^2/m^3)
A	cross-section area (m^2)
C_i	concentration of component i ($kmol/m^3$)
C_t	total concentration, defined in eq. (A.12) ($kmol/m^3$)
D	barrel diameter
E_j	activation energy of reaction j
f_c, f_d	correction factors for the kinetics of polycondensation and degradation reactions, respectively
F_d, F_p	shape factors for drag and pressure flow, respectively
k	mass transfer coefficient for water evaporation (m/s)
k_j	rate constant of reaction j
k_{j0}	rate constant of reaction j at a reference temperature T_0
K_{app}	apparent equilibrium constant of polycondensation reaction
K_1, K_2	constants
h	length of Region I (m)
H	channel length
L	total length (m)
m	number of thread starts
M_n	number-average molecular weight (kg/kmol)
n	number of experimental points
N_r	screw rotation speed (s^{-1})
P	pressure (Pa)
P_r	pressure in Region I (Pa)
P_h	pressure in extruder head (Pa)
Q	volumetric flow rate (m^3/s)
R	ideal gas constant
R_j	rate of reaction j ($kmol/m^3/s$)
RV	relative viscosity
S	residue
T	temperature (K)
T_0	reference temperature (K)
V	volume (m^3)
w	weighting factor for least squares criterion
W	channel width
x_i	weight fraction of component i (kg/kg)
z	down channel position (m)
$\alpha_{i,j}$	stoichiometric coefficient of species i in reaction j
ΔH_{app}	apparent reaction enthalpy
ϕ	pitch angle
η	melt viscosity (Pa·s)
ρ	polymer density (kg/m^3)
τ	average residence time (s)

Subscripts

A	amine end group
c	catalytic
C	carboxyl end group
I	region I
L	amide linkage
M	monofunctional monomer
o	feed
SB	Schiff base
SE	cyclized end group
X	crosslinkage
W	water

REFERENCES

1. C. Tzoganakis, *Adv. Polym. Techn.,* **9,** 321 (1989).
2. U. Berghauss and W. Michaeli, *Kunststoffe,* **81,** 479 (1991).
3. M. Xanthos, Ed., *Reactive Extrusion: Principles and Practice,* Hansen Publishers, Munich, 1992.
4. N. Ogata, *Makromol. Chem.,* **42,** 52 (1960).
5. N. Ogata, *Makromol. Chem.,* **43,** 117 (1961).
6. A. Kumar, R. K. Agarwal, and S. K. Gupta, *J. Appl. Polym. Sci.,* **27,** 1759 (1982).
7. A. Kumar, S. Kuruville, A. R. Raman, S. K. Gupta, *Polymer,* **22,** 387 (1981).
8. D. D. Steppan, M. F. Doherty, and M. F. Malone, *J. Appl. Polym. Sci.,* **33,** 2333 (1987).
9. D. D. Steppan, M. F. Doherty, and M. F. Malone, *J. Appl. Polym. Sci.,* **42,** 1009 (1991).
10. D. D. Steppan, M. F. Doherty, and M. F. Malone, *Ind. Eng. Chem. Res.,* **29,** 2012 (1990).
11. B. R. Choi and H. H. Lee, *Ind. Eng. Chem. Res.,* **35,** 1550 (1996).
12. L. L. Jacobsen and W. H. Ray, *AIChE J.,* **38,** 911 (1992).
13. L. L. Jacobsen and W. H. Ray, *J. Macromol. Sci., Rev. Macromol. Chem. Phys.,* **C32,** 407 (1992).
14. A. H. Hipp and W. H. Ray, *Chem. Eng. Sci.,* **51,** 281 (1996).
15. Z. Tadmor and C. G. Gogos, *Principles of Polymer Processing,* Wiley, New York, 1979.
16. H. E. H. Meijer and P. H. M. Elemans, *Polym. Eng. Sci.,* **28,** 275 (1988).
17. A. R. Vincelette, C. S. Guerrero, P. J. Carreau, and P. G. Lafleur, *Int. Polym. Proc.,* **4,** 232 (1989).

18. B. Siadat, M. Malone, and S. Middleman, *Polym. Eng. Sci.,* **19,** 787 (1979).
19. W. Michaeli, A. Grefenstein, and U. Berghaus, *Polym. Eng. Sci.,* **35,** 1485 (1995).
20. C. Maier and M. Lambla, *Polym. Eng. Sci.,* **35,** 1197 (1995).
21. C. Tzoganakis, J. Vlachopoulos, and A. E. Hamielec, *Int. Polym. Proc.,* **3,** 141 (1988).
22. H. A. Jongbloed, J. A. Kiewiet, J. H. Van Dijk, and L. P. B. M. Janssen, *Polym. Eng. Sci.,* **35,** 1569 (1995).
23. H. A. Jongbloed, R. K. S. Mulder, and L. P. B. M. Jansen, *Polym. Eng. Sci.,* **35,** 587 (1995).
24. J. A. Biesenberger, in *Reactive Extrusion: Principles and Practice,* M. Xanthos, Ed., Hansen, Munich, 1992, Chap. 6.
25. C. A. O. Nascimento, R. Giudici, and N. Scherbakoff, submitted.
26. R. Giudici, C. A. O. Nascimento, I. C. Beiler, and N. Scherbakoff, *Ind. Eng. Chem. Res.,* **36,** 3517 (1997).
27. D. Kahaner, C. Moler, and S. Nash, *Numerical Methods and Software,* Prentice-Hall, Englewood Cliffs, 1989.
28. G. F. Froment and L. H. Hosten, in *Catalysis Science and Technology,* Vol. 2, J. R. Anderson and M. Boudart, Eds., Springer-Verlag, New York, 1981, Chap. 3.